JOURNAL OF KUFA−PHYSICS
journal.uokufa.edu.iq/index.php/jkp/index | ISSN: 2077−5830

Stopping Power of Alpha Particles in Some Human Body Tissues Using Density Functional Theory

Wejdan A. Jasim **Rashid O. Kadhim**

Department of physics, College of Education for Girls, University of Kufa, Najaf, Iraq.

*Corresponding Author E-mail: sitwejdan@gmail.com

ARTICLE INF.

Article history:
Received: 03 JUN., 2023
Revised: 17 OCT., 2023
Accepted: 24 DEC., 2023
Available Online: 29 DEC., 2023

Keywords:

Density functional theory (DFT)
Stopping power calculation,
Human body tissues
Beth's relativistic equation,
Gaussian 09W program.

ABSTRACT

In this research, the stopping power, range, and stop time of alpha particle (He+2) in lung, bladder, intestine, and ovary human tissues are calculated using density functional theory and Beth's relativistic equation in range of alpha particle energy (0.01-1000 MeV). The experimental data of alpha particles extracted from SRIM-2013 program was used for the same human tissues applied in the MATLAB-2021 program, The Mean ionization potential of studied tissues is calculated using Gaussian 09W program. A good agreement has been found between our calculations for stopping power, range, and stopping time of alpha particle in studied human body tissues and SRIM-2013 program calculations.

DOI: https://doi.org/10.31257/2018/JKP/2023/v15.i02.12268

قدرة ايقاف جسيمات ألفا في بعض أنسجة جسم الإنسان كتطبيق للأشعة الطبية باستخدام نظرية الكثافة الوظيفية

وجدان عبد المنعم **راشد عويد كاظم**

جامعة الكوفة،كلية التربية للبنات ، قسم الفيزياء ، النجف ، العراق

الكلمات المفتاحية:

نظرية الكثافة الوظيفية (DFT)،
حساب قدرة الإيقاف
، أنسجة جسم الإنسان
، معادلة بيث النسبية
برنامج كاوسيان W09.

الـــخُـــلاصـــة

في هذا البحث، تم حساب قدرة الإيقاف ومدى وزمن التوقف لجسيم آلفا (He+2) في أنسجة الرئة والمثانة والأمعاء والمبيض باستخدام نظرية الكثافة الوظيفية ومعادلة بيث النسبية في مدى طاقة جسيم آلفا (0.01 -1000 ميغا الكترون فولت). تم استخدام البيانات التجريبية المستخرجة من برنامج SRIM-2013 لجسيم ألفا إلى نفس الأنسجة البشرية المطبقة في برنامج MATLAB-2021، وتم حساب معدل جهد التأين للأنسجة المدروسة باستخدام برنامج Gaussian 09W. تم العثور على اتفاق جيد بين حساباتنا لقدرة الأيقاف والمدى وزمن الإيقاف جسيم آلفا في أنسجة جسم الإنسان المدروسة وحسابات برنامج SRIM-2013.

1. INTRODUCTION

The sopping power and energy dissipation of charged particles through matter has been a subject of great interest for 100 years [1-3] because of its wide areas of application, such as ion implantation, fundamental particle physics, nuclear physics, radiation damage, radiology [2,3]. Heavy charged particles traversing matter lose energy primarily through the ionization and excitation of atoms [4]. The stopping power is defined as the mean energy loss per unit path length–dE/dx. It depends on the charge and velocity of the projectile and, of course, the target material [5,6]. Early investigations of the energy loss of charged particles traversing matter arrive at a general stopping power formula [6]. If an ion beam penetrates matter it loses energy due to collisions with electrons (electronic stopping) and target nuclei (nuclear stopping) [7]. The total stopping power is then just the sum of the stopping powers due to electronic and nuclear interactions [8,9]. At low energies the total energy loss is usually described in terms of electronic stopping power [10]. The nuclear component of the stopping power can be ignored [7]. The possible phenomena that contribute to the electronic stopping is the velocity region well below the light velocity and includes. The momentum exchange in a collision between the ion and a free electron in the target material, the ionization of the ion, the ion captures an electron, the excitation of the ion, the excitation of a target atom, the ionization of a target atom, and the collective effects such as the polarization or the plasmon excitation [9].

2. THEORY

Stopping power of a medium can be defined as the average unit of energy loss suffered by the charge particles per unit path length in the medium under consideration. [11-13]. Stopping power consists of two components: collisions and radiative. The first is the most important for α-particles, resulting from the collision interaction between the incident particles and atomic electrons. The total stopping power can be obtained from SRIM-2003 program [12], which calculates the stopping power and range of ions in matter using a quantum mechanical treatment of ion-atom collision (the manual of SRIM refers to the moving atom as an "ion", and all target atoms as "atom"). A full description of the calculation was given by Ziegler and Biersack [12]. The energy loss in matter has been calculated by many physicists, but the basic, classic derivation was due to Bloch who improved a calculation by Bethe; hence the Bethe-Bloch Formula. The rate of energy loss is given by (–dE/dx); dE/dx being a loss of energy, is a negative quantity. The calculation of dE /dx is done in such a way as to determine the energy deposited in the medium (positive) – hence the explicit negative sign for the loss of energy of the particle. The derivation of the formula is quite long, but we can guess that there are various forms of the formula, which are essentially the same – it just depends on the way particular authors have wanted to parametrize the quantities appearing in the formula. Note that “x”, distance, is not always expressed in meters, but often in units of mass per square meter. This latter parameter comes from multiplying the length by the density of the material. This is a more convenient and useful unit of material thickness as far as experimentalists are considered. The full expression for the Bethe formula can be written as [14]:

$$-\frac{dE}{dx} = \left(\frac{Z_1^* e^2}{4\pi\varepsilon_0}\right)^2 \frac{4\pi Z_2^* \rho_m N_A}{Amc^2}$$

$$\times\left[ln\left(\frac{2mv^2}{I}\right)-ln(1-\beta^2)-\beta^2\right] \quad (1)$$

where Z_1^* effective charge, m electron mass, I mean ionization energy, N_A Avogadro's number, A mass percentage of a mass number, Z_2^* The effective atomic number of the medium , ρ_m mass density, of the stopping material , β = v/c speed of the particle relative to speed of light in vacuum. The effective atomic number Z^* (Z stand for Z_1 and Z_2) may be calculated by the relation [15];

$$Z^*=4\pi\int_{r_b}^{\infty} r^2\,\rho(r)\,dr \quad (2)$$

where r is distance from the nucleus, r_b is determined from Bohr stripping criterion $v \geq bv_F(r_b)=b\hbar[3\pi^2\rho(r_b)]^{1/3}$ where $v_F(r)$ stand for the velocity of Thomas-Fermi orbital of projectile or target atom, b is a constant of proportional about 1.26, and $\rho(r)$ is the electronic charge density distribution in atom. The Lindhard and Scharff theory is gave the effective mean excitation energy I^* as [16];

$$\ln I^*=\frac{4\pi}{Z_2^*}\int_{r_b}^{\infty}\ln\left[\gamma\hbar\omega_p(r)\right]\,r^2\,\rho(r)\,dr \quad (3)$$

where $\gamma=\sqrt{2}$ for $Z \geq 30$, and $\omega_p(r)$ is the local plasma frequency $(4\pi e^2\rho(r)/m)^{1/2}$ Lindhard and Scharff proposed a criterion; $2mv^2 \geq \gamma\hbar\omega_p(r)$, The stopping range (R) is the distance traveled by the incident particle in the target material. In proton therapy, the range magnitudes are also determined as the distance between the starting point of the target's surface and 80% of the Bragg peak. The particle range in the target material can be determined using either the continuous slowing down approximation (CSDA) [17]:

$$R(E)=\int_E^0-\frac{1}{S(E)}dE \quad (4)$$

The stopping time is defined as the time required to stop the charged particle in a medium and it can be calculated from the following integral relationship [18]:

$$t(E)=\int_E^0-\frac{1}{v\,S(E)}dE \quad (5)$$

where v is the ion velocity. Stopping power of composites and tissues is given as sum of stopping powers of its constituent elements according to Bragg equation [19].

$$S_{com.}(E)=\sum_i w_i\,S_i(E) \quad (6)$$

3. Results and discussion

The energy spectrum of the basic elements constituting the tissues taken in this research was obtained by calculating the rate of ionization potential for some tissues of the human body (lung, bladder, intestine, and ovary) and using Gaussian 09W program by using the method of solving (B3LYP) adopted in the functional density theory, which includes the basic aggregates (3-21G, 6-31G, 6-311G, LanL2DZ, LanL2MB, SDD) as in Table 1 Through this method, the rate of ionization effort was extracted for each element, after which the rate of ionization effort for tissues was calculated**.**

TABLE 1: Mean ionization potential of lung, bladder, intestine, and ovary by different basis sets.

Tissue	**Basis sets**					
	3-21G	**6-31G**	**6-311G**	**LanL2DZ**	**LanL2MB**	**SDD**
Lung	137.82	139.60	139.56	129.24	125.01	137.79
Bladder	138.34	140.06	140.01	129.34	125.14	137.32
Intestine	135.56	137.18	137.14	131.69	127.32	136.29
Ova	137	139	139	130.5	126.3	137

ry	.65	.33	.28	6	0	.51

Figure (1-A) represents a comparison between the distribution of the charge of electrons for the studied elements of the human body (lung, bladder, intestine, and ovary) as a function of the ratio of the radial dimension r to the Bohr radius $a_{\circ}$ and through the figure it becomes clear to us that the lowest height is the curve of the hydrogen element, whose electronic arrangement is 1S. For this reason, the density of the charge distribution of the hydrogen element is as low as possible because the center of the shell is distributed in a very large sphere and is estimated at (0.53A), which represents Bohr's radius. As it is clear to us through the figure, the density distribution curves for each element of carbon, nitrogen and oxygen have almost similar curves and the same height with a very small difference. This explains to us that they are from one shell and with the same electronic arrangement 1S2S2P. Therefore, the distribution density is equal for these three elements. While the sodium element has a different height from the rest of the elements, because it has an electronic arrangement 1S2S2P3S. So it has a different behavior in charge distribution density. Sulfur and chlorine have almost identical behavior and heights, and the reason for this is because they have an electronic arrangement 2S2P3S3P. As for the calcium element, we notice through the figure (1-B) that it has the largest charge distribution density and the highest height from the rest of the curves due to the electronic arrangement 1S2S2P3S3P4S which distinguishes it from the rest of the elements in that it has the largest stopping power, as the greater the density of the charge distribution of the element, and the greater the stopping power. The figure (1-B) represents the distribution of the charge density as a function of energy (electron acceleration energy). From this figure, we notice that the energy has an inverse relationship with the radial dimension (i.e. the distance between the particle and the nucleus is as small as possible). In a larger way, the more the tissue shifts towards higher energies, the more stopping power it has. This means that the tissues of the human body resist particles that have larger masses than particles that have small masses.

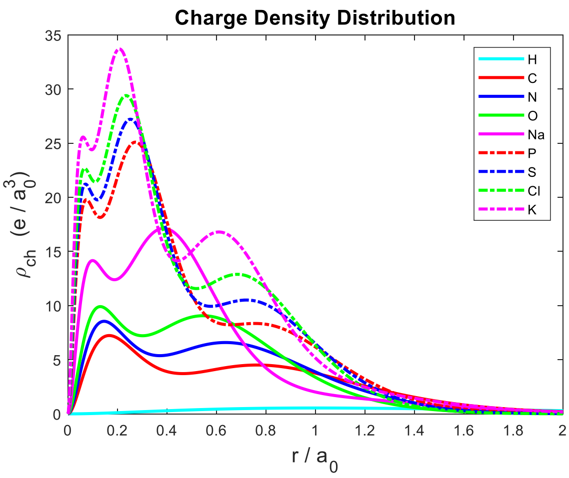

(A)

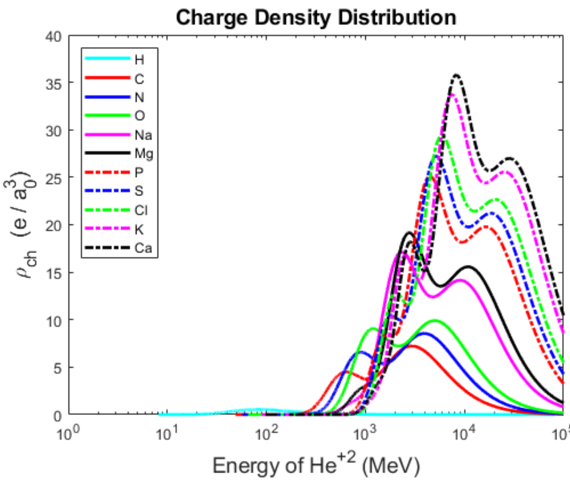

(B)

FIGURE 1 : Charge density distribution of elements in studied human body tissues.

The stopping power of the helium ion was calculated in some of the tissues of the human body (lung, bladder, intestine and ovary) shown in Figure 2. The relationship between the stopping power and the energy of the projectile was plotted, where the black curve was the SRIM global program calculations, and the blue curve was the density functional theory calculations using Beth's theory of relativity through the equation (1), and the red curve represents the matching equation calculations. We can see from the figure that the stopping power of helium in the energy range (2-10 MeV) is large. In lung tissue, it is about 0.5, bladder tissue 0.65, intestine tissue 0.55, and ovarian tissue 0.5, which increases with the increase in the energy of the projectile due to the interaction of the projectile with atomic electron projectiles and the occurrence of ionization and irritation processes for the electrons of the target material to (1000 MeV) due to the projectile passing through the electronic shells because it contains high energy, as we notice through the values of the correlation coefficient that match the practical and theoretical values and that the stopping power decreases with the increase in the mass of the projectile, because the Beth equation calculations are negative in the projectile energy region from 10^{-2} MeV to 10^{-1} MeV for helium in the studied tissues.

TABLE 2: Total stopping power calculations S_{total} for alpha particle (He^{+2}) in studied human body tissues.

Alpha Particle energy (MeV)	S_{total} (MeV cm²/g)			
	Lung	**Bladder**	**Intestine**	**Ovary**
0.01	-335905.37	-336245.65	-334928.12	-336004.49
0.05	-30088.60	-30154.21	-29870.49	-30098.76
0.1	-7056.93	-7089.21	-6943.00	-7059.93
0.5	2298.08	2291.87	2323.14	2298.45
1	1948.12	1945.07	1961.14	1948.51
5	761.56	760.97	764.39	761.73
10	461.51	461.22	462.98	461.62
50	131.26	131.20	131.58	131.29
100	75.02	74.99	75.19	75.04
200	43.08	43.07	43.17	43.09
300	31.43	31.42	31.49	31.43
400	25.31	25.30	25.36	25.32
500	21.52	21.52	21.56	21.53
600	18.94	18.94	18.98	18.95
700	17.07	17.06	17.10	17.07
800	15.65	15.64	15.68	15.65
900	14.53	14.53	14.56	14.54
1000	13.64	13.63	13.66	13.64

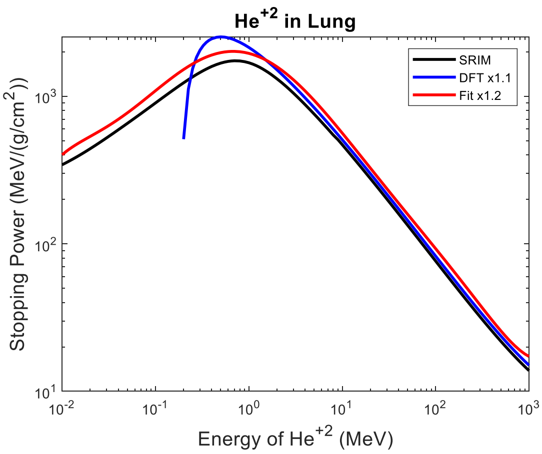

(A) Rc = 0.9779

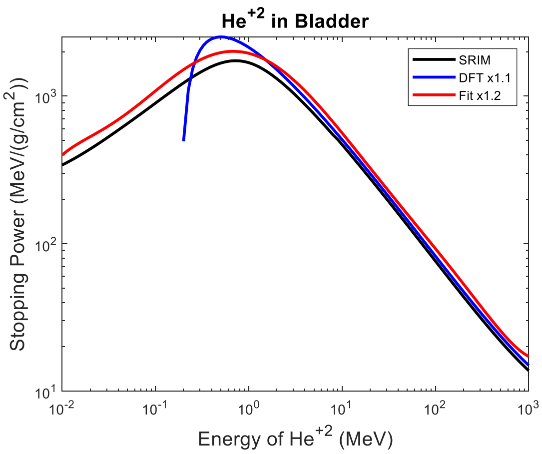

(B) Rc = 0.9776

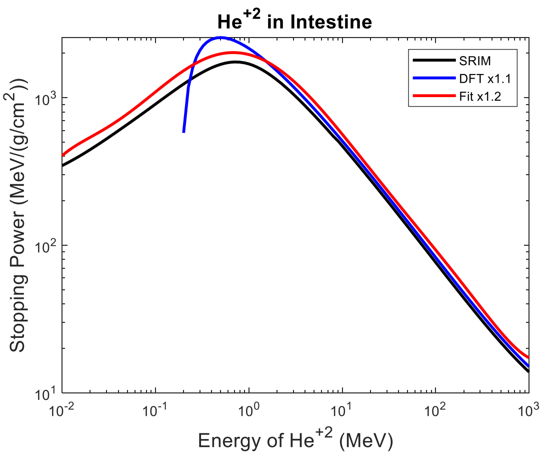

(C) Rc = 0.9784

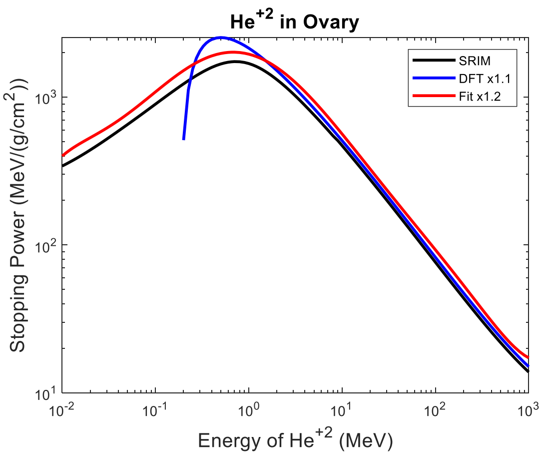

(D) Rc = 0.9778

FIGURE 2: Stopping power calculations for electron in (A) Lung, (B) Bladder, (C) Intestine, and (D) Ovary**.**

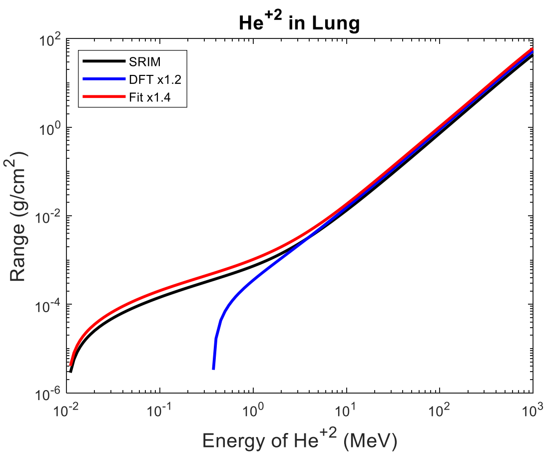

(A) Rc = 0.9999

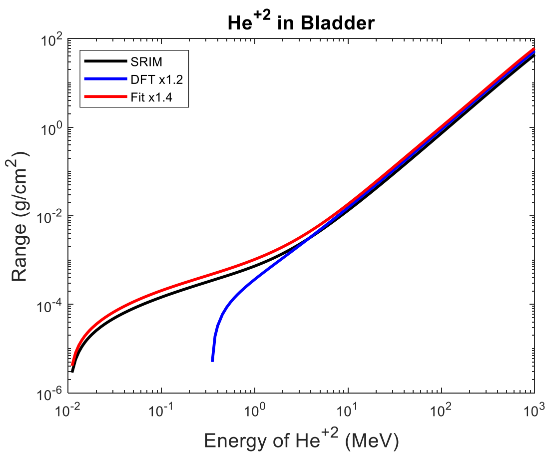

(B) Rc = 0.9999

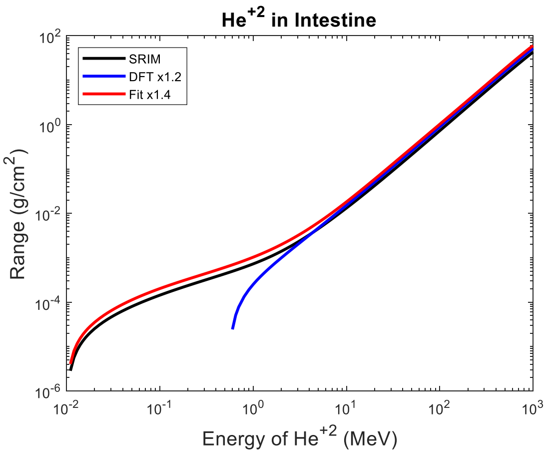

(C) Rc = 0.9999

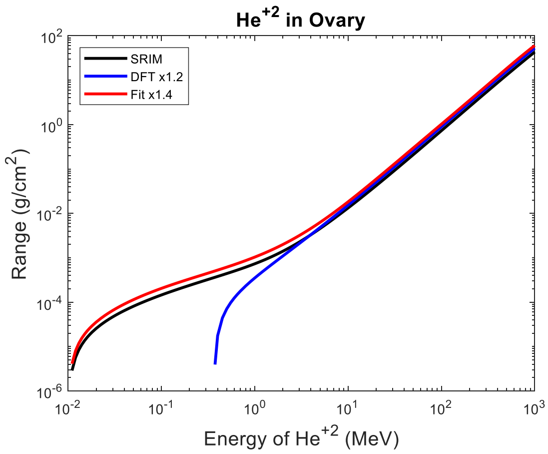

(D) Rc = 0.9999

FIGURE 3: Rang calculations of electron in (A) Lung, (B) Bladder, (C) Intestine, and (D) Ovary**.**

Through the equation (4) and using the numerical method called Trapezoid, the range was calculated for some tissues of the human body (lung, bladder, intestine and ovary), where the black curve represents the calculations of the global program SRIM and the blue curve represents the calculations of the density functional theory and the relativistic Beth equation, while the curve in red represents matching equation calculations. In general, through graphs and figures, the stopping range is directly proportional to the energy of the projectile, and the areas where the Beth equation is negative are the same areas in which the range has negative values. Through the values of the correlation coefficient, we note that the correlation is complete for the range calculations between the global program SRIM and between Beth equation calculations or theoretical calculations at high energies. We also note that there is a curvature in the wake range at high energies due to the presence of an empty area between the atomic shells and the nucleus, so the range grows rapidly. While the slow growth of the range at low energies is caused by the heavy ion interacting with the atomic shells, and after passing through the region of the atomic shells, it freely penetrates the matter, thus increasing and growing the range rapidly and linearly.

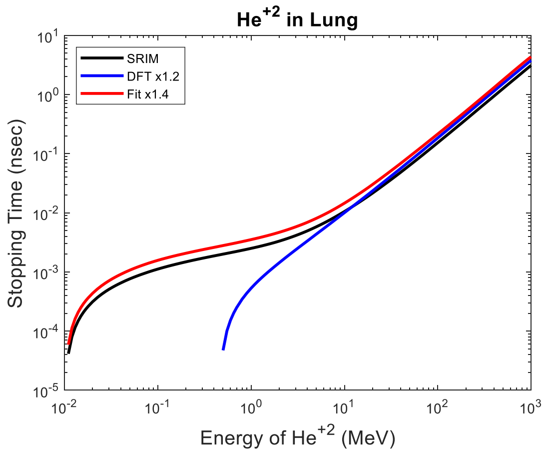

(A) Rc = 0.9999

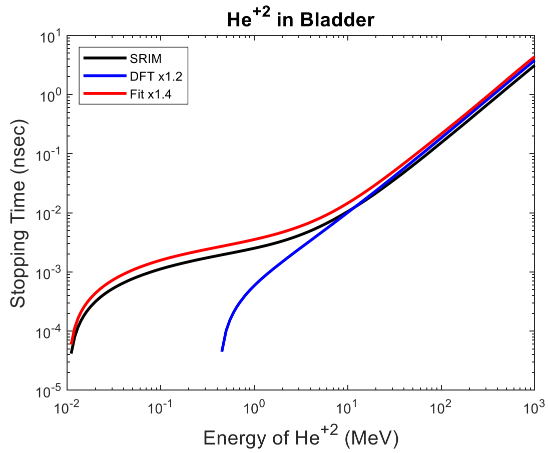

(B) Rc = 0.9999

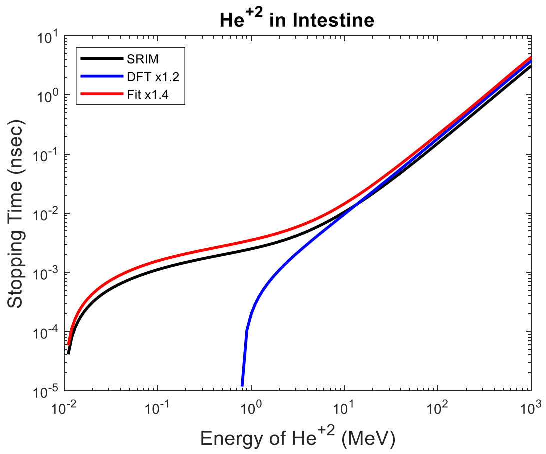

(C) Rc = 0.9999

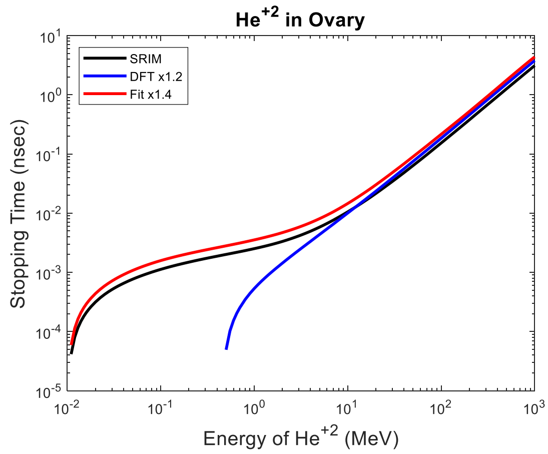

(D) Rc = 0.9999

FIGURE 4: Stopping time calculations of electron in (A) Lung, (B) Bladder, (C) Intestine, and (D) Ovary**.**

Through the equation (5) the suspension time was calculated for some tissues of the human body (lung, bladder, intestine and ovary), where the black curve represents the calculations of the global program SRIM and the blue curve represents the calculations of the density functional theory and the relative Beth equation, while the curve in red represents the calculations of the congruence equation. In general, through graphs and figures, the stopping time is directly proportional to the energy of the projectile, and the areas in which the Beth equation is negative are the same areas in which the stopping time has negative values. Through the values of the correlation coefficient, we note that the correlation is completely for the stopping time calculations between the global program SRIM and between the calculations of Beth's equation or theoretical calculations at high energies. We also note that there is a curvature in the wake-up time at high energies due to the presence of an empty area between the atomic shells and the nucleus, so time grows rapidly. While the slow growth of time at low energies is caused because the heavy ion interacts with the atomic shells, and after passing through the region of the atomic shells, it freely penetrates the matter, thus increasing and growing the range rapidly and linearly.

4. Conclusions

1- The stopping power depends on the charge distribution density, which is inversely proportional to the area. The tissues that have a high distribution density have a large stopping power, unlike tissues that have a low distribution density that has a weak stopping power.
2- The energy is inversely proportional to the dimension, that is, the density of the charge distribution is a function of the energy. The higher the energy of the particle, the less distance between the nucleus and the body, and it has the ability to penetrate the high atom, and thus enables it to penetrate the fabric easily, as it is characterized by being more resistant, as in the element calcium.
3- The relativistic Beth formula based on the density functional theory is good for calculating the stopping power of charged and heavy particles. It increases with an increase in energy by an energy range of (10^{-2} - 10^{3}) MeV due to the interaction of the shell with the atomic shells and the occurrence of ionization and excitation.
4- In general, the energy of the projectile is directly proportional to the range, and the areas in which the calculations of Beth's equation are negative in the stopping power are the same areas that are negative in the stopping range.
5- It was also noted that the calculations of the stopping time in general are directly proportional to the energy of the projectile and The negative area in it is the same as the negative area in the stopping power calculations.

References

[1] J. F. Ziegler, M. D. Ziegler, and J. P. Biersack (2010). SRIM–The stopping and range of ions in matter (2010). Nuclear Instruments and Methods in Physics Research Section B: Beam Interactions with Materials and Atoms, 268(11-12), 1818-1823.
[2] M. J. Berger (1993). ESTAR, PSTAR, ASTAR. A PC package for calculating stopping powers and ranges of electrons, protons and helium ions. Version 2 (No. IAEA-NDS--144). International Atomic Energy Agency.
[3] National Research Council. (1990). Health effects of exposure to low levels of ionizing radiation: BEIR V.
[4] F. A. Mettler, and R. D. Moseley Jr (1985). Medical effects of ionizing radiation, Grune & Stratton. Inc., Orlando, Florida.
[5] S. N. Ahmed (2007). Physics and engineering of radiation detection. Academic Press.
[6] Y. H. Song, and Y. N. Wang (1998). Effects of ion-nucleus sizes on the electronic stopping power for heavy ions in solids. Nuclear Instruments and Methods in Physics Research Section B: Beam Interactions with Materials and Atoms, 135(1-4), 124-127.
[7] W. Brandt, and M. Kitagawa, "Effective stopping-power charges of swift ions in condensed matter", Phys. Rev. B25 (9), 5631-5637, (1982).
[8] L. E. Porter (2003). Further observations of projectile-z dependence in target parameters of modified Bethe–Bloch theory,

International journal of quantum chemistry, 95 (4-5), 504-511.

[9] P. M. Echenique, R. M. Nieminen, J. C. Ashley, and R. Ritchie, (1986). Nonlinear stopping power of an electron gas for slow ions, Physical Review A, 33 (2), 897-904.

[10] J. F. Ziegler (2004). SRIM-2003. Nuclear instruments and methods in physics research section B: Beam interactions with materials and atoms, 219, 1027-1036.

[11] A. Jablonski, F. Salvat, and C. J. Powell (2004). Comparison of electron elastic-scattering cross sections calculated from two commonly used atomic potentials. Journal of physical and chemical reference data, 33(2), 409-451.

[12] F. Salvat, A. Jablonski, and C. J. Powell (2005). ELSEPA—Dirac partial-wave calculation of elastic scattering of electrons and positrons by atoms, positive ions and molecules. Computer physics communications, 165(2), 157-190.

[13] J. G. Hunt, B. M. Dantas, and A. Azeredo (2007). Visual Monte Carlo in-vivo in the CONRAD and IAEA Whole Body Counter Intercomparisons. In Workshop on Uncertainty Assessment in Computational Dosimetry, Bologna.

[14] F. Salvat (2022). Bethe stopping-power formula and its corrections. Physical Review A, 106(3), 032809.

[15] H. Sugiyama (1981). Electronic stopping power formula for intermediate energies. Radiation Effects, 56(3-4), 205–211.

[16] M. C. Tufan, A. Koroglu, and H. Gumus (2005). Stopping power calculations for partially stripped projectiles in high energy region. Acta Phys. Pol. A 107(3), 459–472.

[17] S. M. Kheradmand, and R. Machrafi (2020). Development of a new code for stopping power and CSDA range calculation of incident charged particles, part A: Electron and positron. Applied Radiation and Isotopes, 161, 109145.

[18] J. E. Turner (2008). Atoms, radiation, and radiation protection. John Wiley & Sons.

[19] D. I. Thwaites (1983). Bragg's Rule of Stopping Power Additivity: A Compilation and Summary of Results. Radiation Research, 95(3), 495–518.